Morphology and Cure Kinetics of Unsaturated Polyester Resin/Block Copolymer Blends

N. Boyard, C. Sinturel, M. Vayer, R. Erre

Centre de Recherche sur la Matière Divisée, Unité Mixte de Recherche 6619, 1 B rue de la Férollerie, 45071 Orleans Cedex 02, France

Received 20 June 2005; accepted 26 September 2005
DOI 10.1002/app.23401
Published online in Wiley InterScience (www.interscience.wiley.com).

ABSTRACT: Thermoset blends based on unsaturated polyester and triblock copolymers containing poly(ethylene oxide) and poly(propylene oxide) blocks were investigated. No evidence of self-organization was found. Under our experimental conditions, the block copolymers behaved like classical thermoplastic additives used for shrinkage compensation. According to the type and content of the copolymer, initial systems with one phase or two phases were generated. During curing, except in one case in which thermally induced phase separation was found, reaction-induced phase separation was observed, leading to various types of cured morphologies (cocontinuous or dispersed). For a cocontinuous, two-phase morphology, experimental observations revealed phase separation proceeding via spinodal decomposition frozen in the early stage by gelation. These triblock copolymers appear to be interesting new additives that could be used as good shrinkage compensator additives for industrial applications because it is known that a cocontinuous morphology is needed for this purpose. As for the final morphologies containing dispersed phases, the interpretation of the phenomena occurring upon polymerization requires further investigation. No clear discrimination between spinodal decomposition and nucleation and growth was achieved; in some cases, various successive phase separations were observed. The curing kinetics were examined: an increase in the molar weight and/or copolymer content led to a lower reaction rate. Kinetics curves were modeled by the semiempirical autocatalytic reaction model of Kamal and Sourour with a diffusion-control function. The gelation and vitrification of the system played major roles in the reaction kinetics. © 2006 Wiley Periodicals, Inc. J Appl Polym Sci 102: 149–165, 2006

Key words: block copolymers; kinetics (polym.); morphology; polyesters; thermosets

INTRODUCTION

During curing, an unsaturated polyester (UP) is transformed into a crosslinked network by free-radical copolymerization with a vinyl monomer such as styrene (St), which is the most commonly used. UP/St copolymerization introduces high shrinkage (10%), which induces stresses in the bulk of the cured thermoset material. A thermoplastic additive is added to compensate for the macroscopic shrinkage via porosity formation. The thermoplastic additive (chemical nature, molar weight, proportion in the blend, etc.) strongly influences the final morphology.[1–6]

For miscible (UP/St/thermoplastic additive) blends, the morphology of the cured systems can be described as a compact network of microgels,[5,7–10] which are crosslinked polymer particles on a submicrometer scale; this morphology is the result of a rather complex cure process. UP/St copolymerization increases the molar weight of UP molecules, leading to phase separation (the formation of a thermoplastic-additive-rich phase and a UP-rich phase). This phase separation[11] proceeds until gelation.[4,12–14] The morphology of the cured blend is thus the result of the competition between the reaction rate and the ongoing kinetics of the phase separation.[4,15,16] More explicitly, the nature of the phase separation [spinodal decomposition (SD) or nucleation and growth (NG)] and the time between the onset of the phase separation and the gelation have a great influence on the final morphology.[11,12] Some authors have proposed that the phase separation starts to proceed for a conversion degree lower than 1%[17] and that the gel point occurs at the conversion degree of approximately 5%.[8,10,18–20]

The most efficient thermoplastic additives in terms of the shrinkage compensation and surface aspect are miscible in UP/St blends and lead after curing to a biphasic, cocontinuous structure.[7]

For a few years, there has been growing interest in amphiphilic block copolymers that are able to generate ordered or disordered nanostructures.[21,22] Blending thermosetting resins with these diblock and triblock copolymers has also attracted increasing interest because nanostructured thermoset blends can be obtained.[23,24] Most of the tested blends are composed of epoxy resins[23,24] blended with copolymers contain-

Correspondence to: M. Vayer (marylene.vayer@univ-orleans.fr).

TABLE I
Chemical Characteristics of the Copolymers used in this Study (PEO = E and PPO = P)

Triblock	PEO (wt %)	Chemical composition	M_n (g/mol)	Density (at 25°C)
EPE1	10	$E–P_{17}–E$	1100	1.018
EPE2	10	$E_2–P_{31}–E_2$	2000	1.006
EPE3	40	$E_{13}–P_{30}–E_{13}$	2900	1.050
PEP	40	$P_{14}–E_{24}–P_{14}$	2700	1.048

ing polyethylene, poly(ethylene oxide) (PEO), and poly(propylene oxide) (PPO) blocks. Recently, Zheng et al.[25] demonstrated that PEO is miscible with UP because of hydrogen-bonding interactions. It seems to be quite different for PPO. The use of copolymers containing PEO and PPO blocks as thermoplastic additives could be interestingly examined because PEO and PPO blocks behave differently with UP.

In this article, we thus focus on blends of UP resins and PEO–PPO–PEO and PPO–PEO–PPO copolymers. We examine the influence of the block position and length on the reaction kinetic rate, on the evolution of the morphology during curing, and on the final morphology.

EXPERIMENTAL

Materials

The blends were composed of (1) a UP prepolymer, (2) a curing agent (St), (3) a triblock copolymer, and (4) a polymerization initiator (tertiobutyl perhexanoate ethyl-2).

The UP prepolymer was Palapreg P18-03 from DSM Composite Resins (Schaffhausen, Switzerland) and was made from maleic anhydride, propylene glycol, and neopentyl glycol. The resin P18-03 (density = 1.100 g/cm^3) contained 67.5 wt % UP and 32.5 wt % St. The C═C molar ratio (St/UP) in the blends was adjusted to a value of 2.0 by the addition of St. Tertiobutyl perhexanoate ethyl-2 (1 wt % UP/St) was provided by Peroxide-Chemie GmbH (Pullach, Germany).

Three PEO–PPO–PEO copolymers (named EPE1, EPE2, and EPE3) and one PPO–PEO–PPO copolymer (named PEP) were used in this study as thermoplastic additives. They were provided by Aldrich Chemical Co., Inc. (Saint-Quentin Fallavier, France). The characteristics of these copolymers are listed in Table I. They were used as received, without further purification. The EPE2 and EPE3 copolymers had similar chain lengths of the PPO block in contrast to the PEO blocks. Hence, the influence of the PEO blend miscibility was analyzed. The PEO homopolymer was a semicrystalline polymer with a glass-transition temperature (T_g) of −62°C and a melting temperature (T_m) of 65°C.[26] PPO was amorphous with a T_g of −69°C.

The triblock copolymers exhibited different differential scanning calorimetry (DSC) thermograms, as shown in Figure 1.

DSC scans were carried out from −80 to 50°C at 5°C/min. We determined T_g (taken as the midpoint of the slope change of the heat flow plot) and T_m (determined as the maximum of the endothermic peak). EPE1 and EPE2 had T_g values of −74 and −72°C, respectively. No heat of fusion was detected in these cases; the PEO segments were too short (see Table I). The EPE3 copolymer DSC curve displayed T_g =

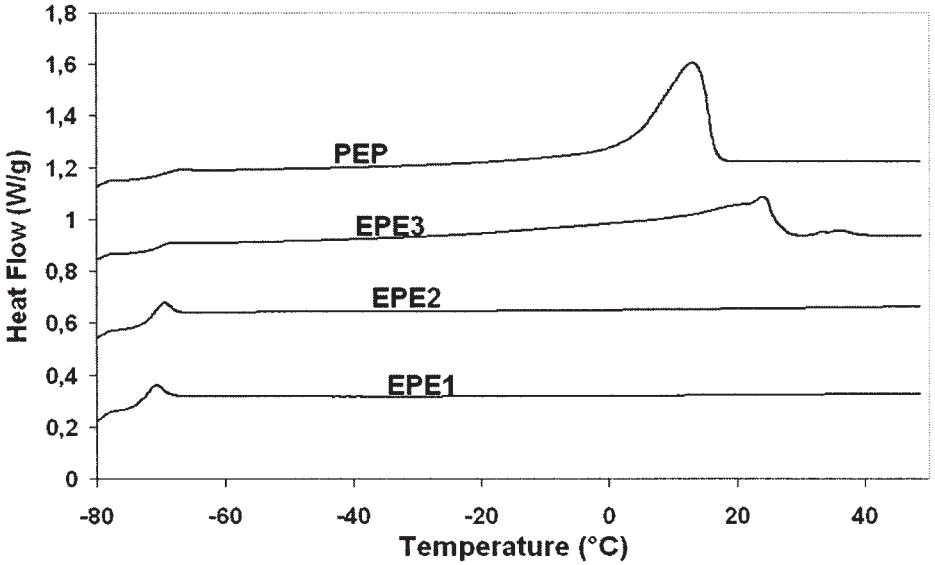

Figure 1 DSC thermograms of the EPE1, EPE2, EPE3, and PEP copolymers. The first scan was from −80 up to 50°C at a heating rate of 5°C/min.

−71°C and two very broad melting peaks (T_{m1} = 24°C and T_{m2} = 35°C). On the basis of a heat of fusion of 205 J/g for 100% crystalline PEO,[26] we estimated the crystallinity degree of EPE3 to be about 22%. Finally, the PEP triblock had T_g = −70°C and a broad melting peak at T_m = 13°C (Fig. 1). The degree of crystallinity of PEP was comparable to that of EPE3 (24.5%).

The UP/St/copolymer blends were made at room temperature; this implies that the block copolymers were in the molten state. All the blends were initially miscible, as judged by their transparent aspect, except for 15% EPE2 and 25% EPE2, for which macroscopic phase separation was visible. Because no T_m and no T_g were observed in the DSC scan for the blends, we can conclude that the addition of the UP resin to a triblock copolymer suppresses its crystallization (when it initially exists).

The copolymer weight contents were 5, 15, and 25% of the ternary blend (UP/St/copolymer). The samples are named by the copolymer content followed by its symbol. For example, a sample containing 15 wt % EPE1 was named 15% EPE1.

Instrumentation and procedures

Sample preparation for the morphology studies

For scanning electron microscopy (SEM) studies, cylindrical samples (diameter = 25 mm, thickness = 3 mm) were molded in a homemade Teflon mold in a preheated 100°C air oven for 15 min. The cured samples were placed in liquid nitrogen for a few minutes to be fractured.

For optical microscopy (OM) observation, a small droplet of the initial blend was introduced between two thin glass coverslips and placed in the hot stage of the microscope; this allowed *in situ* observation of the phenomenon occurring upon polymerization.

DSC

The calorimetric measurements were performed on a PerkinElmer Pyris DSC 6 differential scanning calorimeter (Boston, MA). The instrument was calibrated with indium and dry cyclohexane standards. Dry nitrogen was used as the purge gas, and 15–20-mg samples were analyzed.

To study the copolymerization rate of the blends, the samples were heated from 30 to 160°C at 5°C/min and maintained at that temperature. We verified that at this temperature the curing reaction was complete by conducting a second heating scan up to 200°C and recording no exothermic peak.

Three experiments for each blend were performed to obtain an average value of the exothermic heat of reaction and to verify the reproducibility.

The conversion degree at time t was defined as $\alpha = \Delta H_t/\Delta H_{tot}$, where ΔH_t is the heat of cure at time t and ΔH_{tot} is the total heat of reaction. For the calculation of ΔH_t, we applied a sigmoid curve as a baseline on the exothermic reaction peak because the difference in the calorific capacity (C_P) between the uncured and cured states was not negligible. It was assumed that the change in C_P followed a mixture law $\{C_P(\alpha) = [C_P(\alpha = 0)(1 - \alpha)] + [C_P(\alpha = 1)\alpha]\}$. The sigmoid curve was calculated with an iteration procedure carried out with a Matlab program developed in the laboratory.

Dynamic mechanical analysis (DMA)

The gelation time of the blends was determined by DMA with a Metravib VA3000 apparatus (Limonest, France). The storage shear modulus (G') and loss shear modulus (G'') were continuously measured at 10 Hz under nonisothermal conditions (heating rate = 5°C/min); the crossover of G' and G'' was used to evaluate the position of the gelation. A multiwave experiment was not performed here. As indeed already carefully studied by Van Assche et al.,[19] the criterion used to define the gelation in the case of UPs has little influence on the gelation time because of the sharpness of the transition.

SEM

SEM was carried out on a Hitachi S4200 device combined with an Oxford analyzer controlled by Link Isis software. An electron gun was equipped with a field-emission electron source and was operated at 2 or 5 keV. SEM was performed in the secondary electron mode on carbon-coated fractured samples. Selected samples were etched with methylene chloride for 15 and 30 min to dissolve the thermoplastic phase at the fractured surface for further investigations.

OM

Morphological changes during curing were observed with an Olympus BX51 optical microscope coupled with a Linkam LTS350 heating plate controlled by a Linkam TMS94 controller (possibility of heating and cooling). Images were continuously recorded with a Sony Exwave HAD CCD camera interfaced with Pinnacle Studio version 9 software.

A small droplet of the blend was introduced between two thin glass coverslips and placed in the Linkam sample stage. This stage was then heated from 30 to 160°C at a heating rate of 5°C/min.

RESULTS AND DISCUSSION

Morphology of the systems

SEM observation of the cured systems

The bulk morphology of the cured systems was investigated by SEM on fractured samples. Figures 2–5

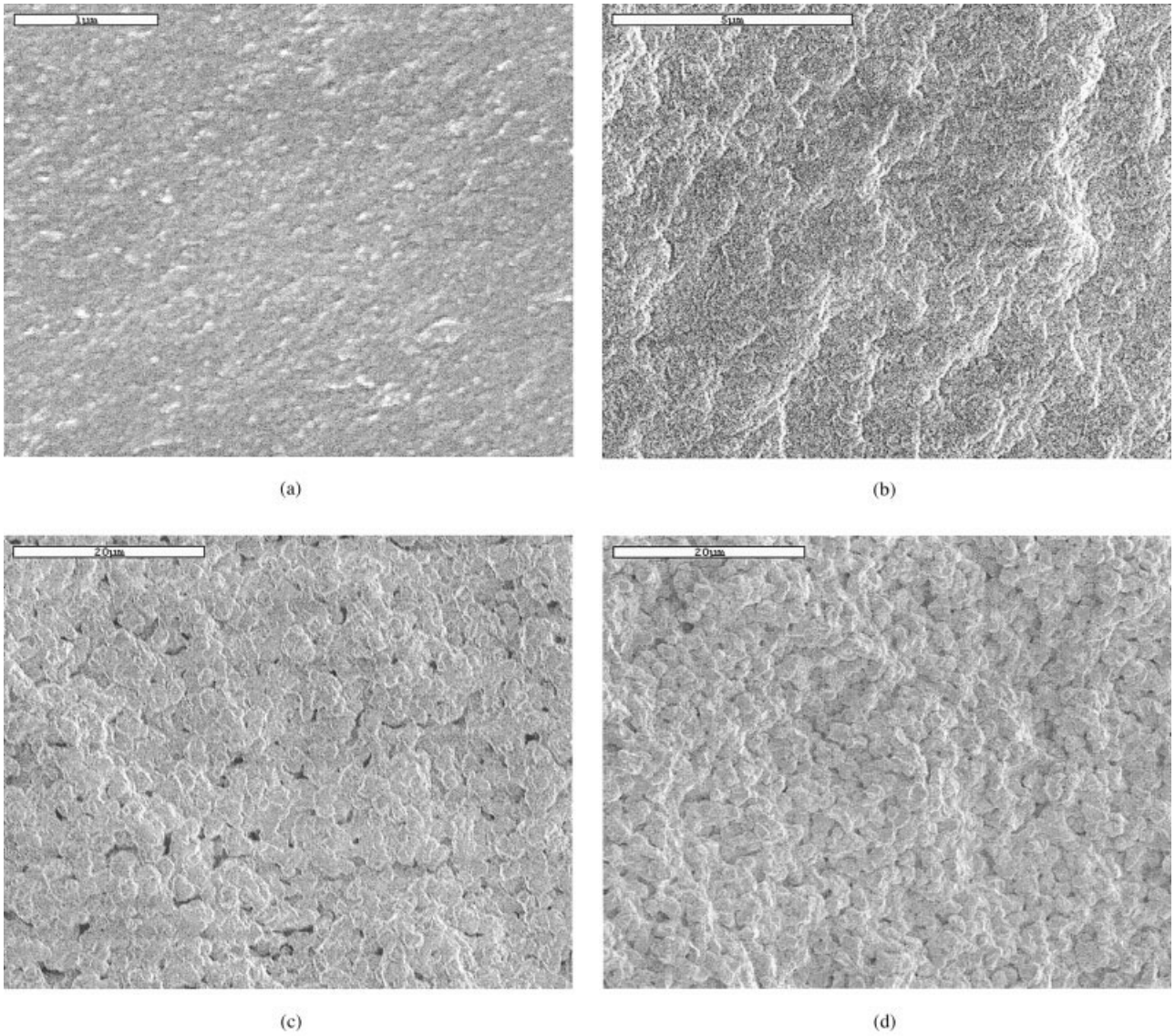

Figure 2 SEM images of fractures of (a) a 5% EPE1 sample (30,000×; scale bar = 1 μm), (b) a 15% EPE1 sample (10,000×; scale bar = 5 μm), (c) a 25% EPE1 sample (2000×; scale bar = 20 μm), and (d) a 25% EPE1 sample after CH_2Cl_2 etching (scale bar = 20 μm).

display the SEM images for the various copolymers at different concentrations. The observed morphologies can be divided into two groups.

The first group exhibits particles on the whole observed surface [e.g., Fig. 2(c)]; 5% EPE1, 15% EPE1, 25% EPE1, 5% EPE2, 5% EPE3, 15% EPE3, 5% PEP, and 15% PEP belong to this group. The size of the particles depends on the type and content of the triblock copolymer. It ranges from a nanometer scale (<500 nm) to a micrometric scale ($\geq$1 μm). Etching samples with CH_2Cl_2 has allowed us to identify the cured phase and the copolymer-rich phase because etching has no effect on the cured phase, whereas the copolymer-rich phase is dissolved. Figure 2(d) shows an example of CH_2Cl_2 etching on 25% EPE1. In comparison with Figure 2(c) (the sample before etching), the particles are slightly smaller and appear more clearly interconnected. Because only the thermoplastic additive has been removed, it can be suggested that the bulk morphology of this group is a three-dimensional network of covalently bonded, cured UP particles surrounded by a thin layer of a copolymer additive. The cured UP phase and block copolymer phase are cocontinuous.

The second group is composed of 15% EPE2, 25% EPE2, 25% EPE3, and 25% PEP. It is characterized by a morphology with a continuous main phase with round, dispersed domains. Etching the sample with CH_2Cl_2 has allowed us to identify all the phases. For 15% EPE2 and 25% EPE2, the main phase is composed of cured UP/St (no particle is visible). The dispersed domains (5–50 μm) are composed of cured particles of UP/St surrounded by the copolymer [Fig. 3(b,c)]. For

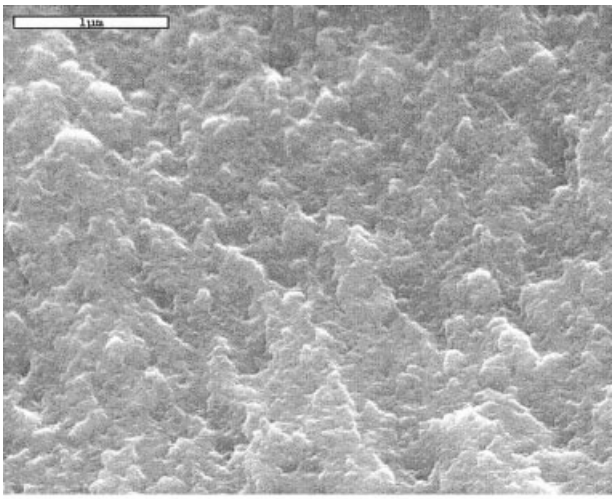

(a)

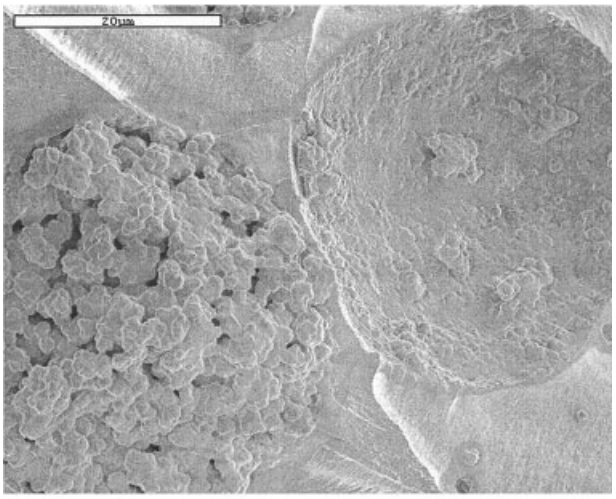

(b)

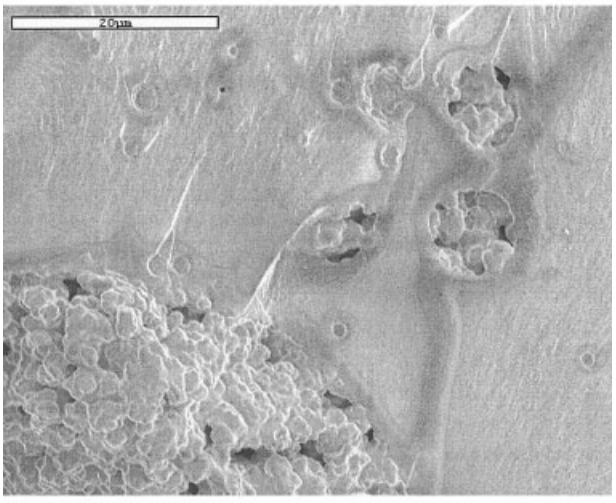

(c)

Figure 3 SEM images of fractures of (a) a 5% EPE2 sample (30,000×; scale bar = 1 μm), (b) a 15% EPE2 sample (2000×; scale bar = 20 μm), and (c) a 25% EPE2 sample (2000×; scale bar = 20 μm).

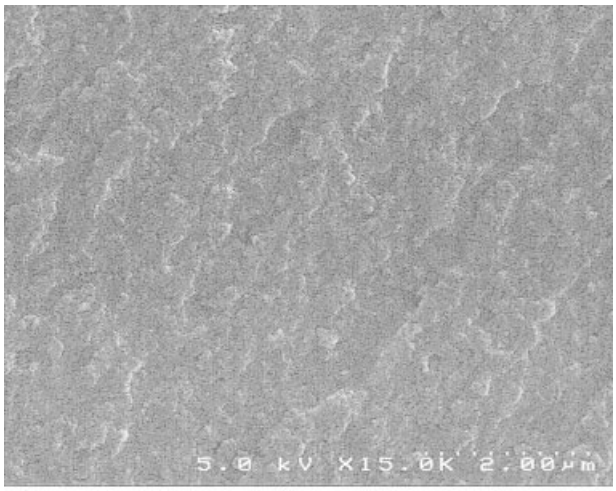

(a)

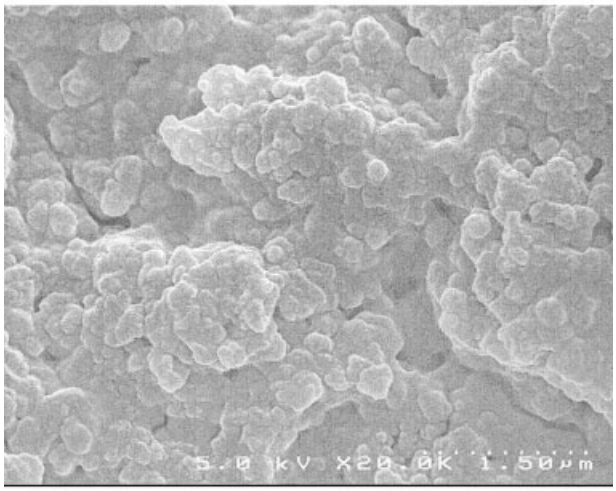

(b)

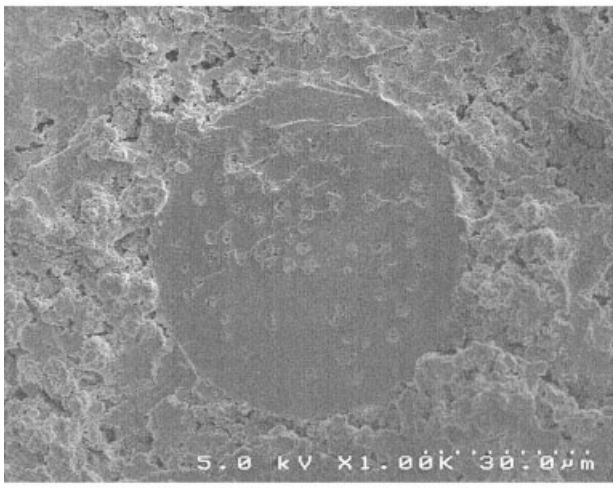

(c)

Figure 4 SEM images of fractures of (a) a 5% EPE3 sample (15,000×), (b) a 15% EPE3 sample (20,000×), and (c) a 25% EPE3 sample (1000×).

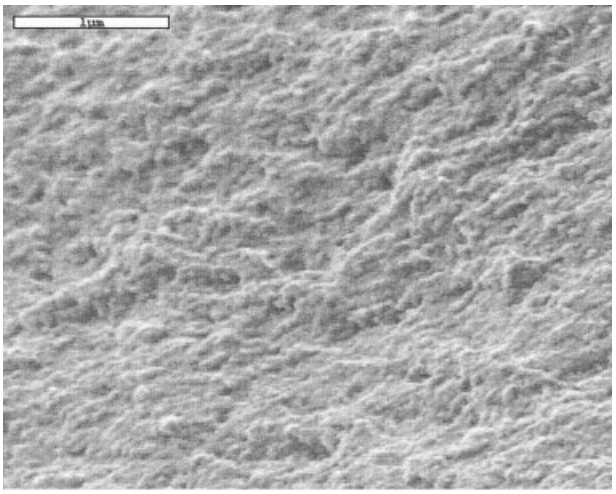

(a)

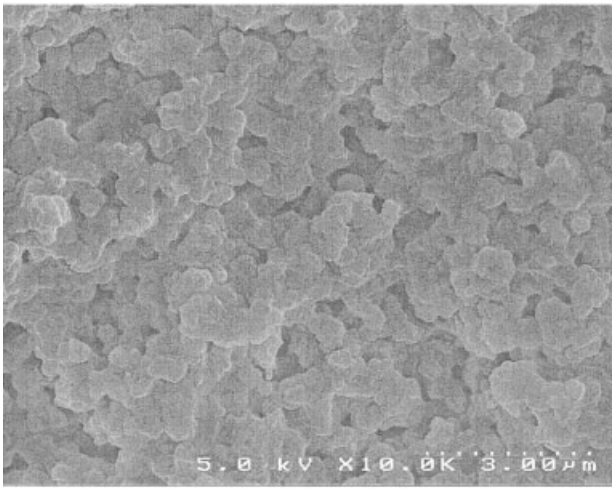

(b)

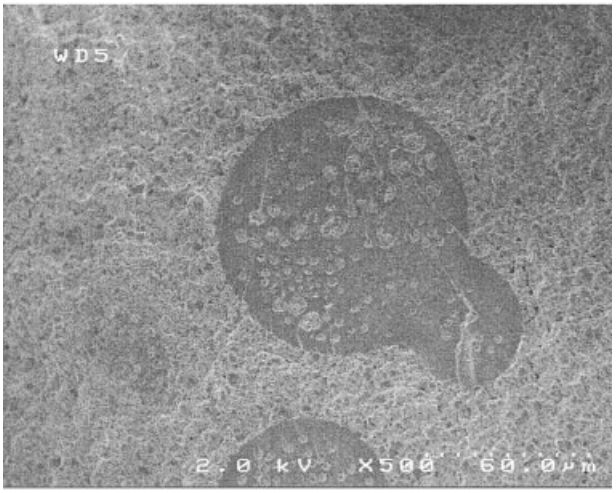

(c)

Figure 5 SEM images of fractures of (a) a 5% PEP sample (30,000×; scale bar = 1 µm), (b) a 15% PEP sample (30,000×), and (c) a 25% PEP sample (30,000×).

25% EPE3 and 25% PEP, the main phase is composed of particles of cured UP/St surrounded by the copolymer. The dispersed domains (10–70 µm) consist of a cured UP/St phase with no visible particles. Within these domains, inclusions are visible [Figs. 4(c) and 5(c)].

Table II (line 1) summarizes the type of structure of the system (cocontinuous or dispersed morphology) revealed by SEM as a function of the type and content of the block copolymer.

Under our experimental conditions, the studied PEO/PPO block copolymers do not lead to cured systems with organized mesophases. These copolymers behave like classical thermoplastic additives used for shrinkage compensation, generating a classical ternary blend (UP/St/block copolymer) ending as a two-phase polymeric system after curing. Interesting new applications of this copolymer can thus be considered as a low profile additive.

In situ observations by OM

Observations by OM are pertinent if the dimensions of the observed objects are within a specific range (>500 nm). Before curing, all the blends appear homogeneous in OM [Figs. 6(a) and 7(a)], except 15% EPE2 and 25% EPE2 [Fig. 8(a)]. These OM observations are obviously correlated to the visual appearance of the blends. Transparent systems were observed to be homogeneous at the scale probed by OM, whereas turbid samples (15% EPE2 and 25% EPE2) exhibited separated domains with sizes ranging from 1 µm to several micrometers. Table II (line 2) displays the initial characteristics of the blends (miscible and nonmiscible). Upon curing, four kinds of behavior were observed in OM.

The first kind of behavior corresponds to samples that are initially homogeneous and are still homogeneous after curing. OM was in this case not adapted to reveal any phenomenon; this is consistent with the SEM images of the cured materials exhibiting domains sizes lower than 500 nm. The blends with this kind of behavior are 5% EPE1, 15% EPE1, 5% EPE2, 5% EPE3, and 5% PEP (see Table II, line 3).

The second kind of behavior corresponds to samples that are initially homogeneous and exhibit a cocontinuous structure with OM after curing (25% EPE1, 15% EPE3, and 15% PEP; see Table II, line 3). As an example, Figure 6(a–c) displays OM observations as a function of the temperature for the 25% EPE1 blend. At the ambient temperature, the blend is homogeneous. When the blend is heated, the system remains homogeneous [Fig. 6(a)] until a first critical temperature (T_{c1}) of 92.5°C. At this temperature, the system becomes heterogeneous, and a characteristic cocontinuous structure appears in the whole sample. For temperatures greater than T_{c1}, no major change is

TABLE II
(1) Characteristics of the cured blends observed by SEM: Cocontinuous (CC) and Dispersed (D); (2) Characteristics of the Initial Blends: Miscible (M) and Nonmiscible (NM); (3) Behavior After Curing Observed by OM (if Visible): CC and D; and (4) Temperature (°C) of the First Onset of Phase Separation Observed by OM (if Visible)

	EPE1			EPE2			EPE3			PEP		
	5%	15%	25%	5%	15%	25%	5%	15%	25%	5%	15%	25%
(1)	CC	CC	CC	CC	D	D	CC	CC	D	CC	CC	D
(2)	M	M	M	M	NM	NM	M	M	M	M	M	M
(3)	—	—	CC	—	D	D	—	CC	D	—	CC	D
(4)	—	—	92.5	—	77.5	79	—	90	61	—	91.5	49

observed: the position of two phases and their relative distances remain identical; only the contrast between the two phases increases [Fig. 6(b)]. When the temperature reaches a second critical temperature (T_{c2}) of 112.5°C, black areas with a dendritic structure start to develop [Fig. 6(c)]. These areas correspond to pores.

The third kind of behavior corresponds to initially homogeneous samples that exhibit after curing a heterogeneous structure with separated domains. Two blends exhibit this kind of behavior (25% EPE3 and 25% PEP). Figure 7(a–c) displays the example of 25% PEP. The sample becomes heterogeneous at T_{c1} (49°C). Spherical, separated domains are observed for temperatures greater than T_{c1} [Fig. 7(b)], and the characteristics of the system evolve continuously (the position and size of the separated domains). A second phase separation occurs in the main phase at T_{c2} (66.5°C). Figure 7(c) shows OM observations for temperatures greater than T_{c2}. Pores are observed at higher temperatures.

The fourth kind of behavior is observed for 15% EPE2 and 25% EPE2 and corresponds to initially heterogeneous blends ending as cured, heterogeneous structures. Figure 8(a,b) displays the behavior of 15% EPE2. In this system, one phase becomes heterogeneous at T_{c1} = 77.5°C, whereas the other phase remains homogeneous.

Discussion

For polymer blends, phase separation can be generated either by a temperature [thermally induced phase separation (TIPS)] or by a chemical reaction [reaction-induced phase separation (RIPS)]. Phase separation takes place when a blend initially in the one-phase region of the phase diagram reaches the two-phase region of the diagram. Under our experimental conditions, phase separation can be induced either by temperature or by polymerization because curing is performed during a continuous increase of the temperature. To distinguish between these two phenomena, we examined by OM the behavior during heating of all the studied blends containing no polymerization initiator. All these blends (except 25% PEP) appear to be stable upon heating in the studied range of temperatures. This suggests that the aforementioned phase separations are due to UP/St copolymerization and related variations of the system characteristics (the component concentration, interaction parameters, and entropy). For the 25% PEP blend containing no polymerization initiator, phase separation was observed at 49°C suggesting in this case TIPS.

For both TIPS and RIPS, two types of phase-separation mechanisms can be involved. Depending on the quench depth, SD or NG[12] can be observed. The NG mechanism is encountered when the system is quenched into the metastable region of the phase diagram. It results in spherical, dispersed domains, the size of which increases with time. The SD mechanism takes place if the mixture is quenched deeply into an unstable zone of the phase diagram. Small and periodic fluctuations of the composition give birth to a three-dimensional, cocontinuous morphology that forms during the early stage of the SD phase separation (step 1); this first step is described by the linearized Cahn–Hilliard–Cook theory.[27–30] The structure tends to increase in size (step 2), and after this self-similar growth, cocontinuity is lost; this leads to fragmented particles (step 3) and then spherical particles (coarsening process, step 4). As a result, the latest stage of phase separation can be described in the two cases (NG and SD) as spherical, dispersed particles. Discrimination between NG and SD can thus only be achieved if we consider the first stage of the phase separation as a cocontinuous structure is formed only in SD. This first stage generally proceeds extremely quickly, and the observation is not easy. However, gelation can interact in some cases with the phase-separation mechanism by quenching the mechanism leading to a system frozen in the first step of phase separation;[31,32] 25% EPE1 illustrates this behavior. During polymerization, a cocontinuous, two-phase morphology is observed that can be attributed to the first step of SD. As the structure remains the same upon curing, without any structure size increase and without any coarsening, it can be proposed that the growth of the structure is in that case prematurely interrupted by gelation. This assumption is consistent with the gelation temperature (T_{gel}) extracted from the

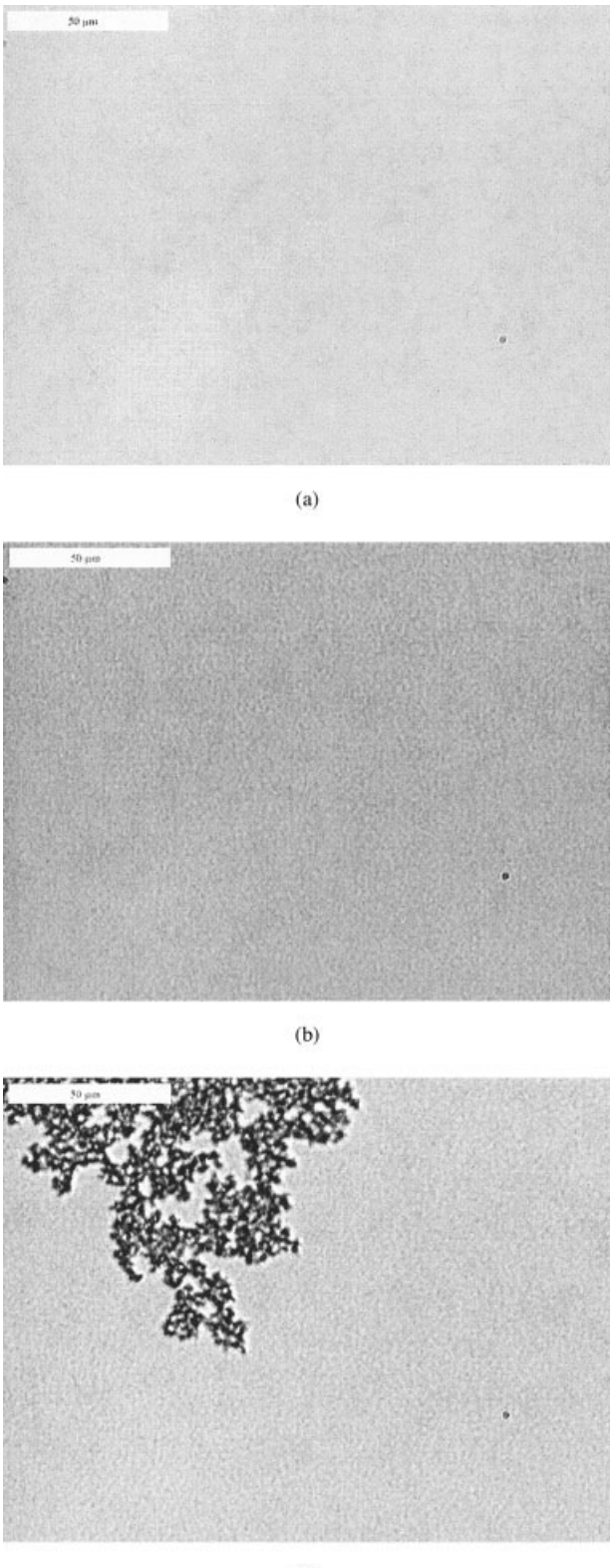

Figure 6 OM images (500×) of a 25% EPE1 blend under curing: (a) the initial blend (scale bar = 30 μm), (b) the blend at 105°C (scale bar = 50 μm), and (c) the blend at 115°C (scale bar = 30 μm).

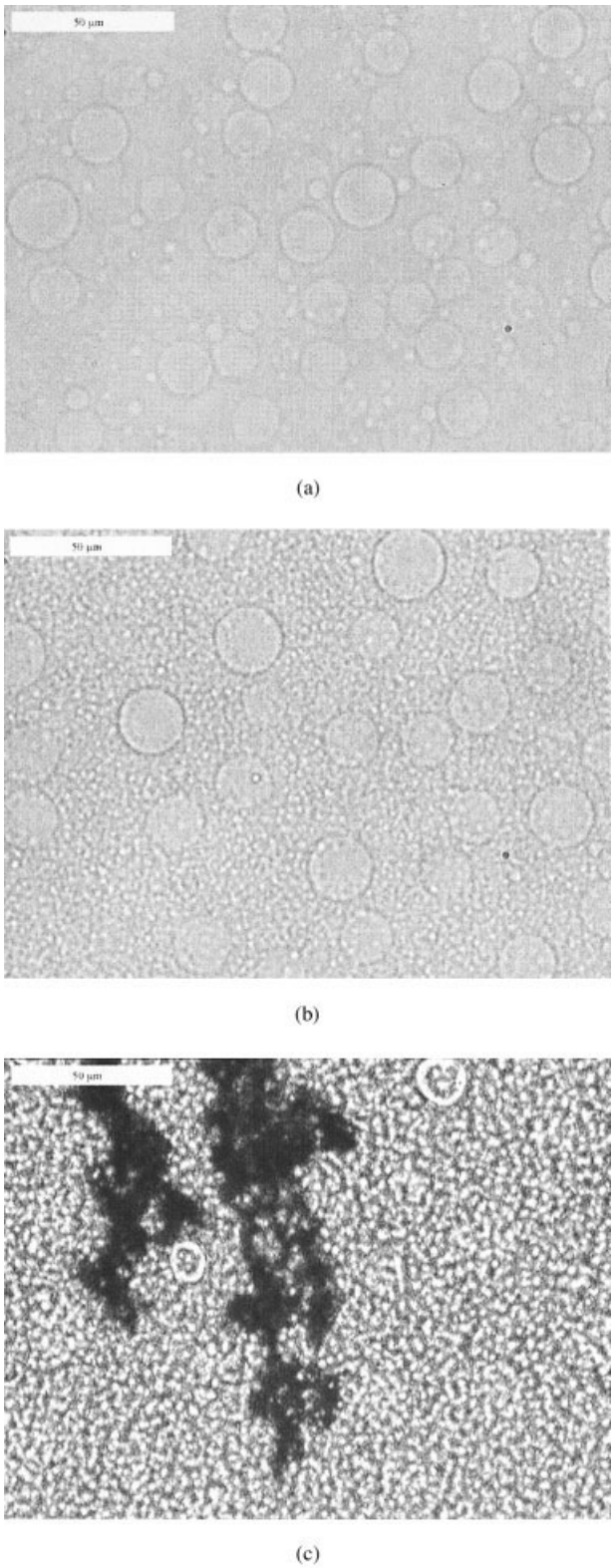

Figure 7 OM images (500×) of a 25% PEP blend under curing: (a) the initial blend (scale bar = 50 μm), (b) the blend at 58°C (scale bar = 50 μm), and (c) the blend at 70°C (scale bar = 50 μm).

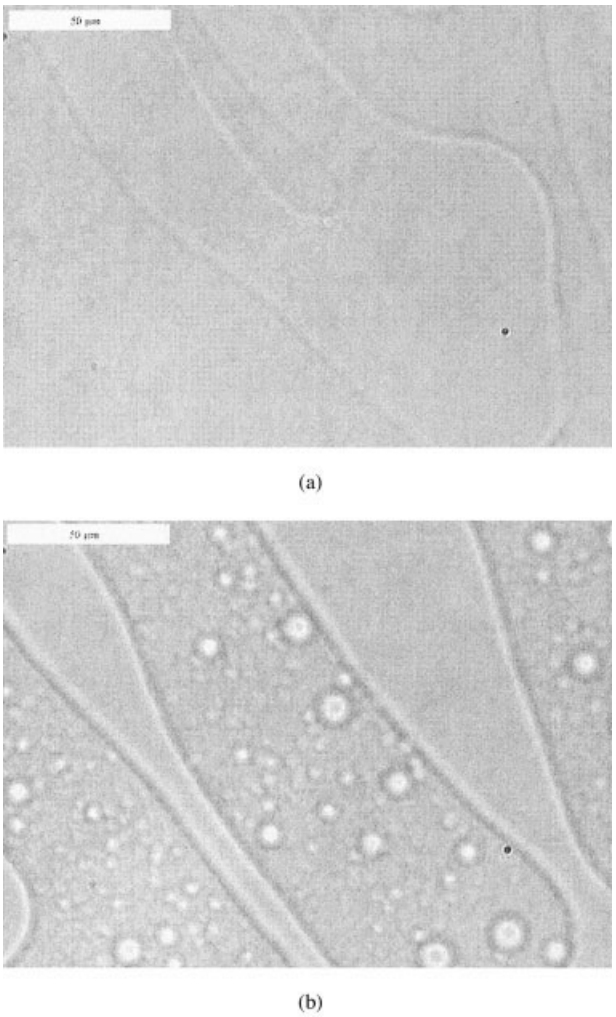

Figure 8 OM images (500×) of 15% EPE2 under curing: (a) the initial EPE2 (scale bar = 50 μm) and (b) EPE2 at 80°C (scale bar = 50 μm).

DMA experiments under the same conditions of the temperature scan used for OM observations. For 25% EPE1, the onset of phase separation was evaluated to be 92.5°C from the OM observations, and T_{gel} was evaluated to be 93°C for DMA experiments. To confirm the existence of correlation distances within the material in this case, chord distribution was performed. The use of chord distributions allows us to characterize a medium[33,34] (random medium, correlated medium, etc.). For that purpose, raw OM images were converted into binary images imposing a gray-level threshold. Figure 9 displays a OM binary image for cured 25% EPE1. One phase appears in white, and the other one appears in black. Chord distributions were been performed on the binary images and are shown in Figure 10. Correlation peaks can be observed for the two phases; this is typical of a correlated medium.[34] This is consistent with our assumption concerning the development, in this system, of periodic fluctuations of the concentration, which are typical of the first step of SD. The correlation peaks can be observed around 1.0 μm for the white phase and around 0.8 μm for the black phase. Interestingly, these values are rather similar to the dimensions of the particles observed in SEM, suggesting that the phase separation imposes the final morphology. Similar behaviors have been observed for 25% EPE1, 15% EPE3, and 15% PEP. Table II (line 4) gives the values of T_{c1} in each case. T_{gel} is close to 93°C for all the cases. We propose to extend this mechanism (frozen SD) to other systems (5% EPE1, 15% EPE1, 5% EPE2, 5% EPE3, and 5% PEP) for which OM is not able to point out any phenomenon upon polymerization but for which SEM has revealed similar cured structures.

For all the other cases, the interpretation of the phenomena is not straightforward. It indeed involves in a first-step formation of spherical domains, the size of which varies as a function of time (1–50 μm). A second phase separation occurs in some cases. As demonstrated previously, NG and also SD can be involved as gelation does not interact with the first step of the phase separation, allowing the phase separation to proceed until a later stage. The onset of phase separation is indeed observed in these cases for low temperatures (see Table II, line 4) far away from T_{gel} (ranging from 90 to 93°C in all cases). The unambiguous interpretation of all these complex phenomena needs in these cases further investigations such as time-resolved scattering experiments in which discrimination between SD and NG can be achieved.

Each behavior originates from the characteristics of the initial phase diagram (governed by the chemical structure of the block copolymer, which influences its affinity with the thermosetting polymers) and the position of the system in this phase diagram (governed by the content of the block copolymer). PEO blocks show good interactions with the UP prepolymer (an interaction parameter of −1.29 and hydrogen bonding

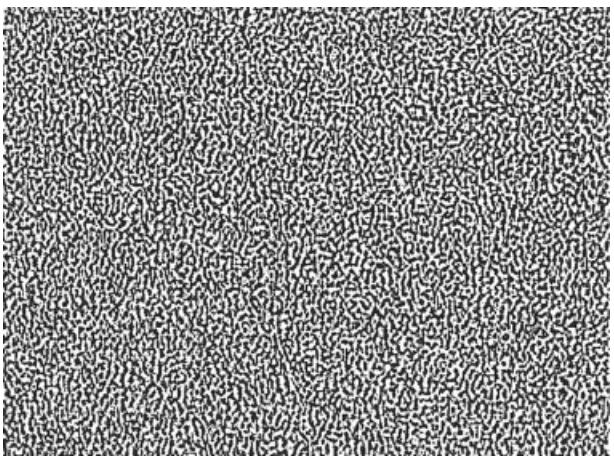

Figure 9 Corresponding digitalized OM image of cured 25% EPE1 (before pore formation at 110°C).

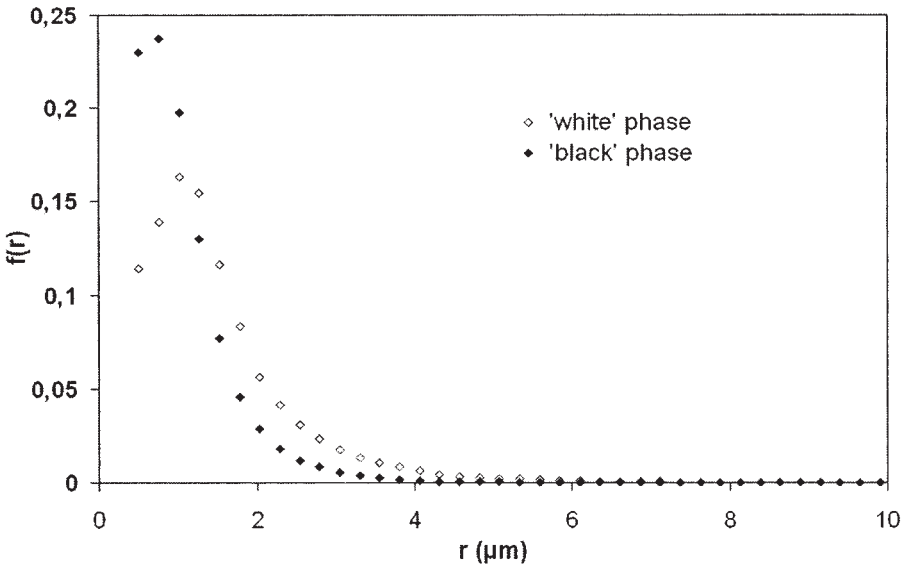

Figure 10 Chord distribution in the two phases revealed by digitalization of Figure 9.

have been reported in the literature[25]), whereas PPO and UP tend to separate. As a result, one key parameter for miscibility is the relative lengths of the PEO and PPO blocks in the copolymer. A good illustration can be found by a comparison of the behavior of 15% EPE2 and 15% EPE3. These two additives have similar PPO block lengths but different PEO block lengths. The 15% EPE2 blend with a shorter PEO block is heterogeneous, whereas the 15% EPE3 blend with a longer PEO block is homogeneous. To confirm the role of PEO and PPO in the blend miscibility, we investigated separately the behaviors of the PEO and PPO segments. For this purpose, PEO and PPO oligomers with a number of structural units close to the one of the EPE3 copolymer [600 (E_{13}) and 1000 g/mol (P_{30}), respectively] were used and added in UP/St at concentrations (6% for PEO and 9% for PPO) equivalent to those in 15% EPE3. The blend containing PEO was homogeneous in the studied temperature range, whereas the system with PPO was heterogeneous under the same conditions. Furthermore, the position of the block is fundamental. With the same molar weight and the same proportion of PEO, the miscibility of EPE3 and PEP is very different because for 25 wt % copolymer blends, phase separation has a TIPS origin for PEP and a RIPS origin for EPE3. Eventually, all the systems containing EPE1 are initially miscible despite a high ratio of the PPO length to the PEO length. This particular behavior can be attributed to the low molecular weight of this additive.

Kinetic studies

Kinetics of the reaction during heating and evolution of the conversion degree

DSC measurements were carried out for all the blends. Figures 11 and 12 display plots of the reaction rate versus the temperature for blends containing the EPE1copolymer and EPE2 copolymer. The curves for all the blends exhibit rather similar shapes with first an induction period in which no reaction is observed. When the temperature is high enough to ensure a sufficient concentration of free radicals, the reaction rate starts to increase continuously, reaches a maximum, and then decreases. Such behavior results from the constant increase of the temperature (thermal activation of the propagation reaction) superimposed on the autocatalytic nature of the reaction. The copolymerization of UP with St is indeed a typical free-radical crosslinking reaction involving three main steps (initiation, propagation, and termination) and is accompanied by a Trommsdorf effect[35] (autocatalytic reaction). This phenomenon is characterized by a dramatic increase in the reaction rate followed by a decrease of this rate and can be explained by the control of the termination rate by diffusion. At the beginning of the reaction, a pseudo-steady-state period is observed (essentially for isothermal conditions): the initiation rate is equivalent to the termination rate. At intermediate conversions, the specific rate of termination becomes controlled by diffusion and then decreases, whereas the free-radical concentration increases. Consequently, the overall reaction rate exhibits a steep rise and goes through a maximum. For higher conversion degrees, the depletion of monomers combined with a large restriction (imposed by diffusion) on the specific rate of propagation leads to a rapid decrease of the reaction rate.

The effect of the block copolymer concentration can be seen in Figures 11 and 12. Increasing the concentration of the copolymer slows down the reaction rate for the system containing either EPE1 or EPE2. This can be explained by the dilution effect of the copoly-

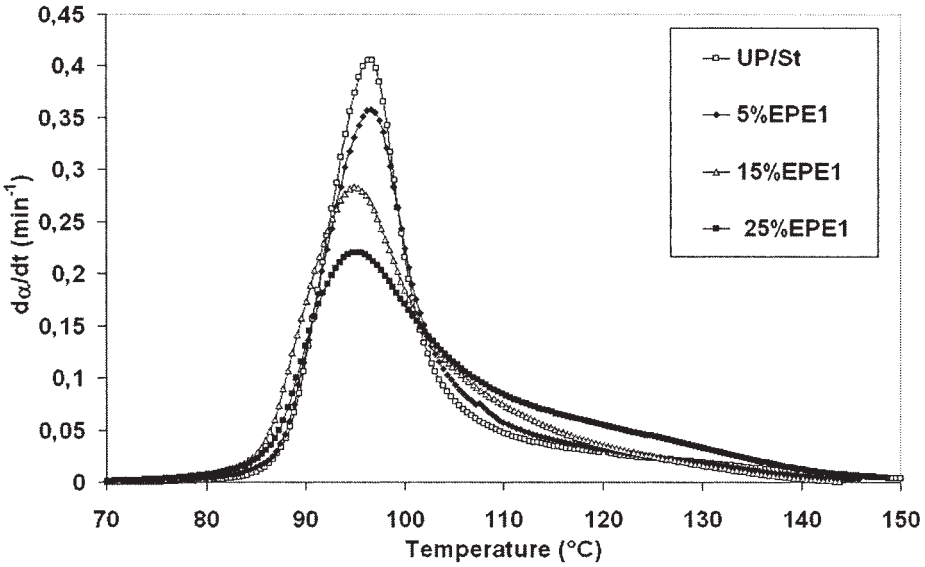

Figure 11 Reaction rate ($d\alpha/dt$) versus the temperature for UP/St and UP/St blends containing EPE1 at a heating rate of 5°C/min.

mer, which implies a lower probability of the crosslinking reaction. Similarly, the nature of the block copolymer has a strong effect, as shown also in Figure 13. For a given concentration of the block copolymer, increasing the molar weight slows down the reaction. This can be explained by the fact that when the reaction proceeds, the thermoplastic phase will phase-separate out and then modify the reaction rate.

For the highest copolymer block concentrations (15 and 25%), a peculiar behavior can be observed. The curves (Figs. 11–13) present a shoulder (the reaction rate decreases more slowly) at 108–110°C. This feature is characteristic of successive vitrification/devitrification of the sample, indicating that T_g of the system has reached a value equal to the sample temperature.[36]

Table III displays the reaction enthalpy for all the samples. Except for 25% EPE2, for the same UP/ST mass, the addition of a block copolymer has no significant impact on the reaction heat: a degree of cure of 1 has been attained for all the samples after curing (Fig. 13). A lower value can be observed for 25% EPE2 (Fig. 13). This blend is initially immiscible and presents a phase separation that gives birth to dispersed domains. In this case, the change in the morphology,

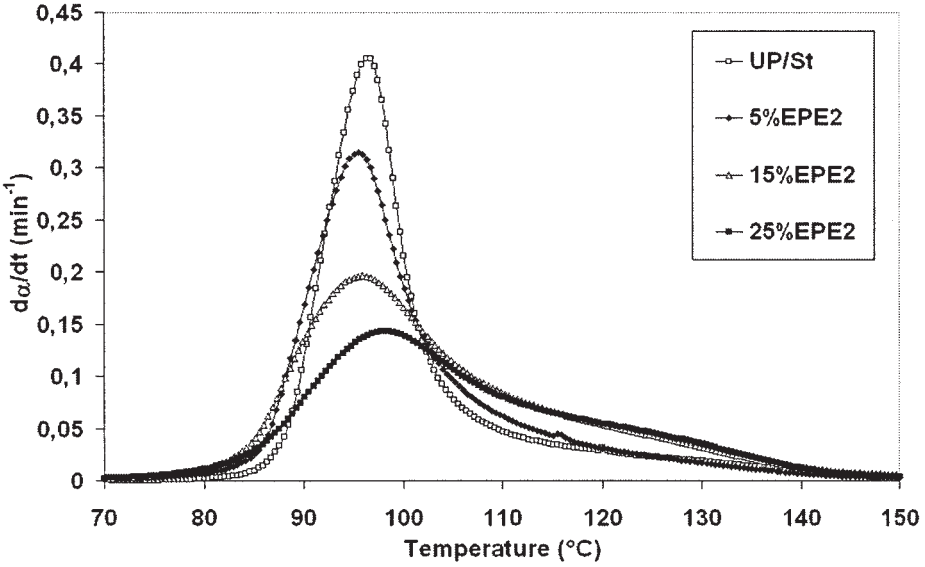

Figure 12 Reaction rate ($d\alpha/dt$) versus the temperature for UP/St and UP/St blends containing EPE2 at a heating rate of 5°C/min.

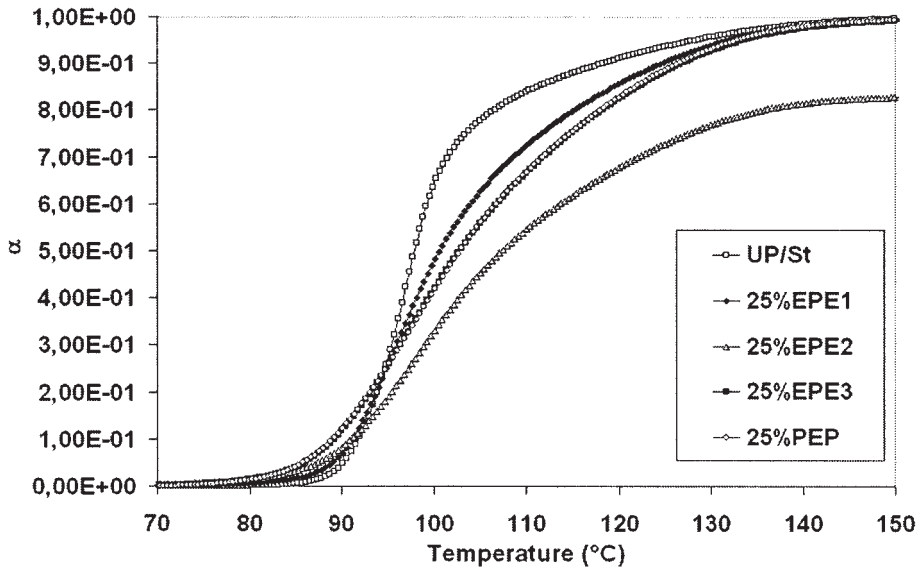

Figure 13 Nonisothermal DSC curing profiles at 5°C/min for UP/St systems blended with copolymers (25 wt %).

which is induced by a larger amount of the additive and thus a variation of the blend miscibility, is correlated to a final degree of curing lower than 1.

Kinetic analysis of the curing reaction

Plotting the reaction rate versus the conversion degree allows us to highlight some changes in the blend crosslinking induced by physicochemical phenomena. Figures 14–17 show the reaction rates versus the conversion degree for blends containing EPE1, EPE2, EPE3, and PEP under nonisothermal condition of heating. All the curves display a rather classical shape for the whole range of conversion degrees, which is characteristic for an autocatalytic reaction.

However, all the curves present two inflexion points. First, a rather broad inflexion point can be observed on the curves for conversion degrees ranging from 7 to 11% before the maximum reaction rate is reached (located in the 35–40% conversion degree range). Finally, the curves fall strongly before a second inflexion point (ca. 60% conversion), after which the reaction rate decreases more slowly.

As the curing reaction is deeply influenced by physicochemical phenomena occurring meanwhile, we propose to attribute the first inflexion point to gelation and the second inflexion point to the onset of the vitrification/devitrification phenomenon.

To confirm the origin of the first inflexion point, we determined when gelation occurred. From the crossover of G' and G'', T_{gel} was extracted from the DMA experiments (an example is given in Fig. 18) and converted to the conversion degree on account of the DSC curves. Gelation was attained for conversion degrees ranging from 9 to 10% for all the blends. Our results are consistent with the literature, in which the conversion degrees of gelation have been reported within the first percent of the reaction for UP resins.[10,37] As observed in Figures 14–17, the position of the gel point obtained by DMA corresponds to the first inflexion point. The slow rise of the reaction rate after this first inflexion point is induced by two antagonist phenomena. On the one hand, the temperature catalyzes the crosslinking (i.e., the reaction rate rises more quickly), but on the other hand, the extent of cure favors kinetics more and more controlled by diffusion of the species (i.e., a slower reaction rate). Combining all these physical changes, one can explain the large maximum observed. After the maximum, the decrease of the rate of curing is justified by the depletion of monomers combined with a larger restriction (imposed by a

TABLE III
Enthalpy of Reaction (ΔH_R)

Blend composition	(%)	$\Delta H_R \pm 10$ (J/g)	ΔH_R (J/g) for a UP/St mass of 1 g
UP/St		337	337
EPE1	5	331	347
	15	300	352
	25	265	351
EPE2	5	340	357
	15	301	358
	25	225	300
EPE3	5	332	349
	15	298	343
	25	259	345
PEP	5	336	353
	15	300	345
	25	272	340

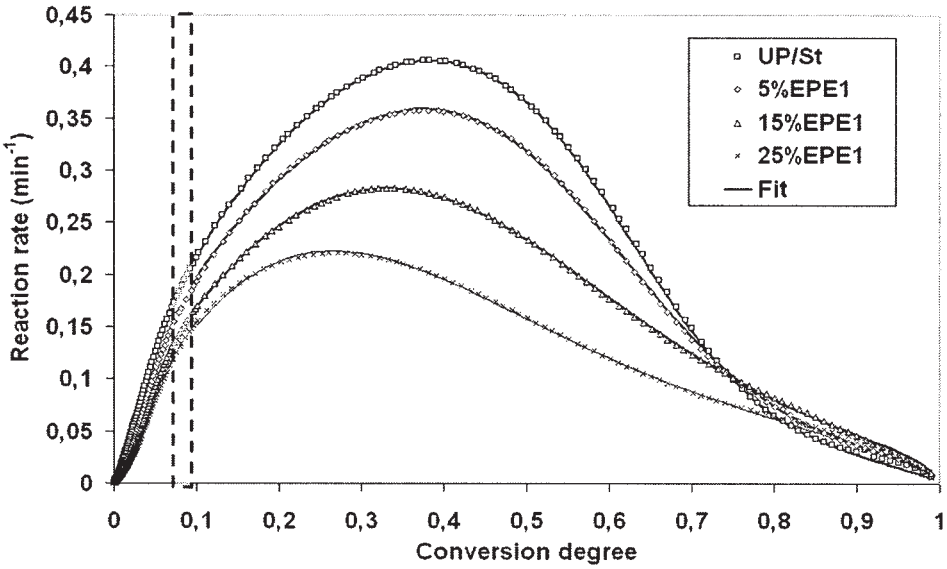

Figure 14 Reaction rate versus the conversion for UP/St and UP/St blends containing EPE1: experimental data and fitted data.

larger diffusion control) on the specific rate of propagation.

The second inflexion point is observed for a relatively high conversion degree (60% on average). During the polymerization, T_g of the thermoset polymers continuously evolves because of the continuous chemical transformation up to a total crosslinked polymer. The vitrification of such reacting thermosetting system occurs when T_g reaches the reaction temperature. For highly reactive systems (e.g., UP resins) and/or when the applied heating rate is sufficiently small, vitrification occurs under nonisothermal conditions (it also happens under isothermal conditions). The reaction then proceeds under mobility-restricted conditions and stops quickly. However, devitrification is observed when the reaction temperature again surpasses T_g of the vitrified resin. A succession of vitrification and devitrification is represented on the curve of the reaction rate by a shoulder.[36,38]

Modeling the kinetics of the reaction

As mentioned previously, curing is complex because of the interaction between kinetics induced by the

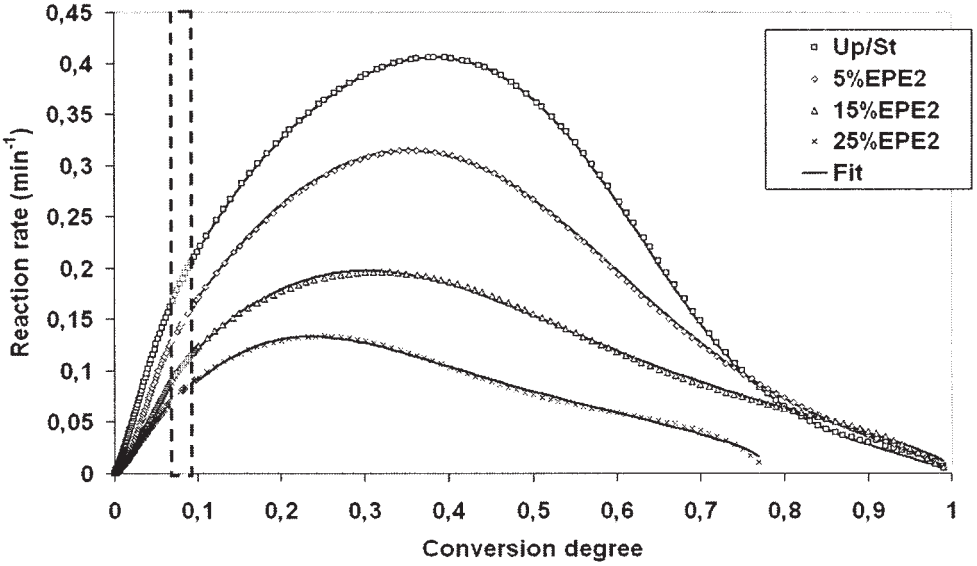

Figure 15 Reaction rate versus the conversion for UP/St and UP/St blends containing EPE2: experimental data and fitted data.

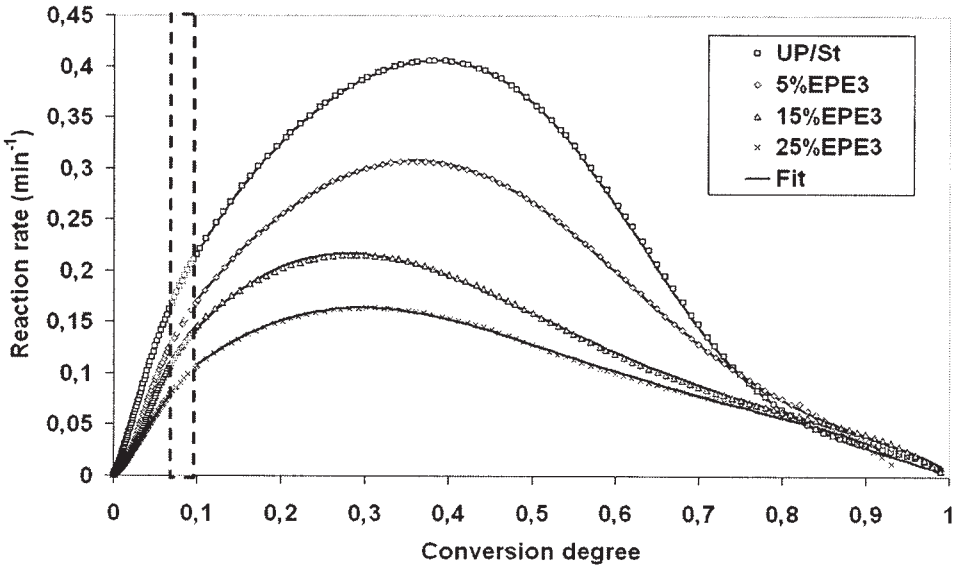

Figure 16 Reaction rate versus the conversion for UP/St and UP/St blends containing EPE3: experimental data and fitted data.

reactivity of species and physicochemical phenomena that happen during curing. Phase separation, gelation (i.e., morphological modifications), and vitrification are the most important.[8,19,36,39] During curing, the kinetics evolve from kinetics controlled by the chemical reactivity of species to kinetics controlled by the diffusion of reacting species in the medium.

The modeling of the reaction kinetics can be divided essentially into two classes of models. The first ones are based on polymerization mechanisms,[40,41] whereas the second ones are phenomenological. Taking into account the complex nature of the kinetics described previously, modeling procedures described in the literature use general phenomenological models[36,42–44] (*n*th-order, autocatalytic mechanisms with diffusion control or not).

One of the most popular empirical models is from Kamal and Sourour;[42] it was successfully applied for the first time by those authors to UP/St blends. It has been used for other thermosetting polymers and especially for epoxy resins.[43–45] A chemically controlled kinetic reaction rate can be modeled as follows:

$$\frac{d\alpha}{dt} = (k_1 + k_2\alpha^m)(1 - \alpha)^n$$

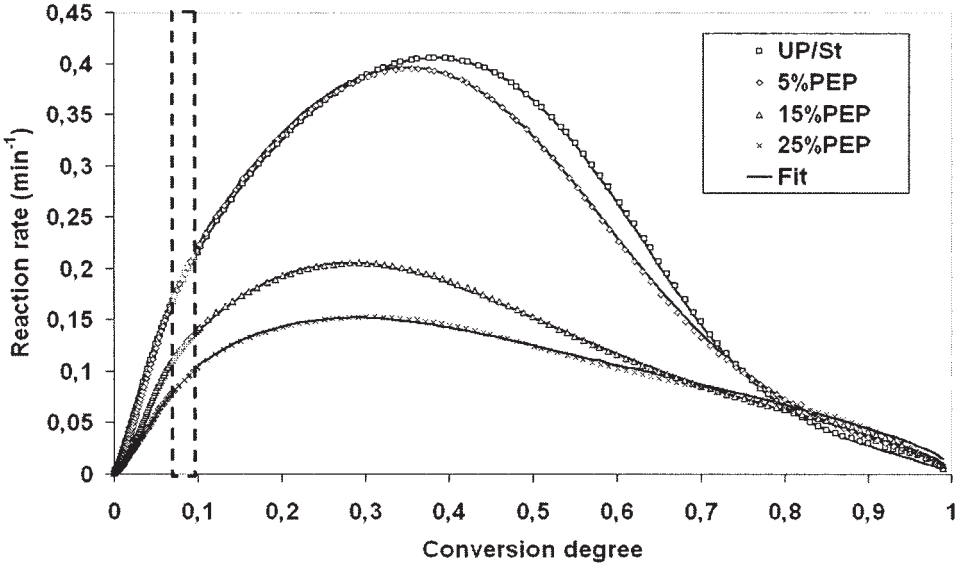

Figure 17 Reaction rate versus the conversion for UP/St and UP/St blends containing PEP: experimental data and fitted data.

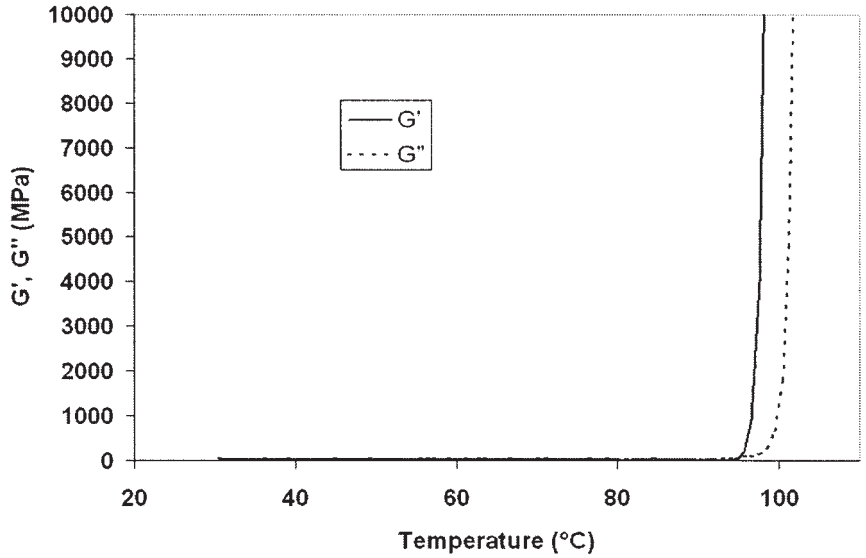

Figure 18 G' and G'' as functions of the temperature for an initially uncured system (5% EPE2).

where α is the fractional conversion at time t, k_1 and k_2 are rate constants, m and n are kinetic exponents of the reaction, and $m + n$ gives the overall reaction order. Kinetic constants k_2 and k_1 depend on the temperature according to an Arrhenius law. This equation can be used for modeling both isothermal and nonisothermal experiments.[36]

In our case, k_1 was found to be negligible, and the reaction rate could be written as follows:

$$\left(\frac{d\alpha}{dt}\right)_{\text{chem}} = k_c(T)\, f(\alpha) \tag{1}$$

$$k_c(T) = A_c \exp\, -\frac{\mathrm{E_a}}{RT} \tag{2}$$

where A_c is the pre-exponential factor, E_a is the activation energy, R is the gas constant, and T is the absolute temperature. After gelation, the reaction is controlled by the diffusion. To take into account this phenomenon, eq. (1) is modified by a diffusion-control function [$f_d(\alpha)$], which considers the reduced molecular mobility due to the network formation process. Equation (3) is thus obtained:

$$\frac{d\alpha}{dt} = \left(\frac{d\alpha}{dt}\right)_{\text{chem}} f_d(\alpha) = k_c(T)\, f(\alpha)\, f_d(\alpha) = k_e(T,\alpha)\, f(\alpha) \tag{3}$$

The empirical overall rate constant (k_e) is often described by the Rabinowitch model.[20,43,44] It is written as follows:

$$\frac{1}{k_e} = \frac{1}{k_c} + \frac{1}{k_d} \tag{4}$$

where k_d is the rate constant for diffusion-controlled kinetics.

The introduction of eq. (4) into eq. (3) yields

$$\frac{d\alpha}{dt} = \frac{k_c(T) k_d(T,\alpha)}{k_c(T) + k_d(T,\alpha)} f(\alpha) \tag{5}$$

$$f_d(\alpha) = \frac{k_d(T,\alpha)}{k_c(T) + k_d(T,\alpha)} \tag{6}$$

A semiempirical expression of the diffusion rate constant was proposed by Chern and Poehlein[46] and is defined as follows:

$$k_d(T,\alpha) = k_c(T)\, \exp[-C(\alpha - \alpha_c)] \tag{7}$$

where C is an adjustable parameter and α_c is the critical value of the conversion degree for which diffusion becomes the controlling factor. By introducing eq. (7) into eq. (6), we obtain an expression of $f_d(\alpha)$:

$$f_d(\alpha) = \frac{1}{1 + \exp[C(\alpha - \alpha_c)]} \tag{8}$$

The mathematical form of $f_d(\alpha)$ expresses a gradual diffusion-controlled reaction rate. Therefore, there is an α range in which both the diffusion and chemical reactivity of species control the kinetics. When α is much smaller than α_c, the diffusion effect is negligible, and $f_d(\alpha)$ is approximately unity. As α increases, $f_d(\alpha)$ decreases and slowly approaches zero, at which the reaction is strongly affected by the vitrification/devitrification phenomenon.

To describe the reaction rate, parameters C, α_c, A_c, E_a, m, and n were determined without any constraints

TABLE IV
Constants of the Modified Autocatalytic Model

Blend	(%)	A_c (min^{-1})	E_a (J/mol)	m	n	$m + n$	C	α_c (%)
UP/St		3.5×10^{11}	8.1×10^4	0.56	1.08	1.64	10.6	65
EPE1	5	2.8×10^{11}	8.1×10^4	0.49	0.85	1.34	9.0	62
	15	1.5×10^{11}	7.9×10^4	0.51	0.85	1.36	6.0	51
	25	0.8×10^{11}	7.5×10^4	0.70	1.00	1.70	4.8	30
EPE2	5	2.4×10^{11}	8.0×10^4	0.58	1.12	1.70	7.1	60
	15	3×10^{11}	8.1×10^4	0.55	0.95	1.50	5.3	35
	25	2.4×10^{11}	7.9×10^4	0.75	0.6	1.35	6.8	12
EPE3	5	2.8×10^{11}	8.1×10^4	0.50	0.95	1.45	7.5	60
	15	2.1×10^{11}	7.9×10^4	0.60	0.95	1.55	5.2	30
	25	2.8×10^{11}	8.2×10^4	0.40	0.60	1.00	5.7	32
PEP	5	2.4×10^{11}	8.0×10^4	0.55	0.95	1.50	8.3	59
	15	2.3×10^{11}	8.0×10^4	0.52	0.92	1.44	5.3	33
	25	2.5×10^{11}	8.0×10^4	0.50	0.90	1.40	4.0	8

on them by the minimization of criterion J, which is defined as follows:

$$J = \sum_{x=1}^{N} \left(\left(\frac{d\alpha}{dt} \right)_{\exp,x} - \left(\frac{d\alpha}{dt} \right)_{\mathrm{mod},x} \right)^2 \qquad (9)$$

where $(d\alpha/dt)_{\exp,x}$ is the xth point of the experimental curve and $(d\alpha/dt)_{\mathrm{mod},x}$ is the xth point of the modeled curve.

The reaction rates for blends containing EPE1, EPE2, EPE3, and PEP were fitted with the presented models. Before gelation, the curves were fitted with eq. (1). After gelation, the control of the reaction by diffusion was taken into account, and the curves were fitted with eq. (3).

Figures 14–17 show the reaction rates versus the conversion degree for EPE1, EPE2, EPE3, and PEP and the corresponding fits (for $\alpha \geq 10\%$). The fits are in good agreement with the experimental data in most cases. The range of conversion degrees in which a change in the kinetics is observed (it is a result of gelation) is indicated on the graph.

The fitting parameters are given in Table IV. The E_a values remain in the same range whatever the blend composition is. A_c exhibits a smaller value for all the blends containing copolymers in comparison with UP/St. This indicates that the reaction rate is slower for the copolymer blends than for UP/St. The overall reaction order ($m + n$) is in the range of 1.0–1.7. The lowest values are obtained for 25% EPE2 and 25% EPE3. At α_c, the curing reaction becomes mainly controlled by the diffusion ($f_d = 0.5$). α_c decreases when the copolymer content increases. Plots of $f_d(\alpha)$ versus α for UP/St and EPE1 blends are shown in Figure 19. $f_d(\alpha)$ decreases because of the gradual control by the

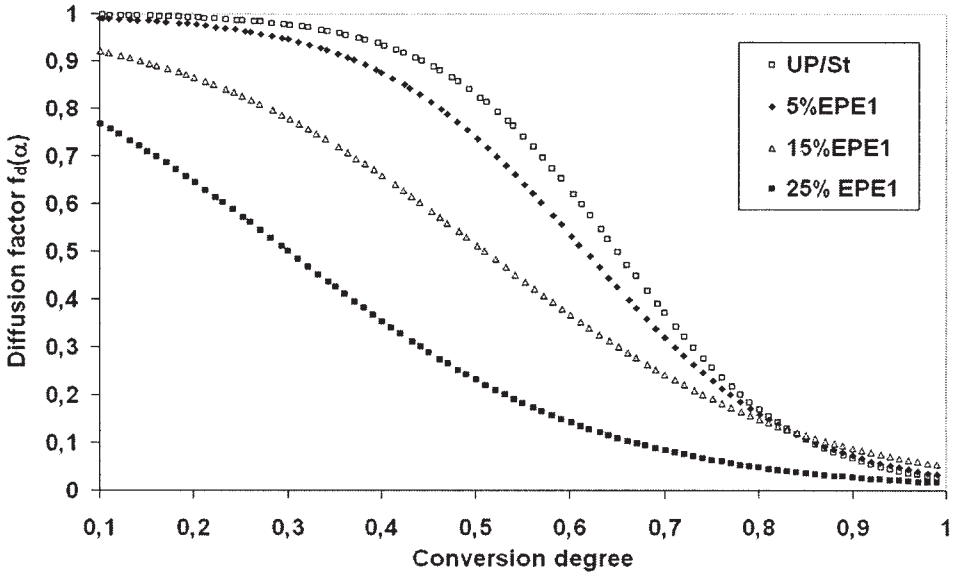

Figure 19 $f_d(\alpha)$ versus the conversion degree for UP/St and various concentrations of EPE1.

diffusion of the reaction rate. A comparison of the curves shows that an increase in the copolymer content in the blend leads to an earlier decrease in the diffusion factor. For low α values (as early as 10%), the diffusion factor of 25% EPE1 is less than 1. Similar results were obtained with other blends.

CONCLUSIONS

Under our experimental conditions, the studied PEO/PPO block copolymers do not lead to cured systems with organized mesophases. These copolymers behave like classical thermoplastic additives used for shrinkage compensation, generating classical ternary blends (UP/St/block copolymer). We have demonstrated that various morphologies (cocontinuous or dispersed) can be obtained by the selection of the appropriate type (relative amounts of PEO and PPO blocks) and/or amount of the copolymer. Experimental evidence of phase separation proceeding via SD frozen in the early stage by gelation has been obtained for the cocontinuous systems. For the dispersed morphologies, the interpretation of the phenomenon occurring upon polymerization is more ambiguous and needs further investigation. Time-resolved small-angle laser light scattering or small-angle X-ray scattering (depending on the size of the domains) will be carried out for this purpose.

The influence of the block copolymer on the kinetics of polymerization has also been investigated. DSC measurements demonstrate that the rate of polymerization of UP decreases when the block copolymer is added. The dilution of the reactant seems not to be the only involved factor. A pronounced control of the reaction by diffusion has been revealed after the gelation point, which occurs at conversion degrees lower than 10%, by the modeling of the rate of reaction by a semiempirical autocatalytic model of Kamal and Sourour. This behavior can be tentatively related to the phase separation occurring in the blends that deeply modifies the characteristics of the system. However, despite a broad variety of morphologies generated upon curing, the effect of the various block copolymers on the kinetics is found to be rather similar. The relation between the phase-separation process and the kinetics is, as a result, not straightforward. In all cases, vitrification appears to play an important role in the kinetics and has to be taken into account when the rate of reaction is modeled.

The authors thank Annie Richard from the Microscopy Center and Menzolit for providing the unsaturated polyester resins.

References

1. Huang, Y.-J.; Jiang, W.-C. Polymer 1998, 39, 6631.
2. Huang, Y.-J.; Su, C. J Appl Polym Sci 1995, 55, 323.
3. Suspene, L.; Gerard, J.-F.; Pascault, J.-P. Polym Eng Sci 1990, 30, 1585.
4. Li, W.; Lee, L. J. Polymer 2000, 41, 697.
5. Serré, C.; Vayer, M.; Erre, R.; Boyard, N.; Ollive, C. J Mater Sci 2001, 36, 113.
6. Bucknall, C. B.; Davies, P.; Partridge, I. K. Polymer 1985, 26, 109.
7. Vayer, M.; Serré, C.; Boyard, N.; Sinturel, C.; Erre, R. J Mater Sci 2002, 37, 2043.
8. Yang, Y. S.; Lee, L. J. Polymer 1988, 29, 1793.
9. Funke, W.; Okay, O.; Joos-Müller, B. Adv Polym Sci 1998, 136, 139.
10. Hsu, C. P.; Lee, L. J. Polymer 1993, 34, 4496.
11. Kieffer, J.; Hedrick, J. L.; Hilborn, J. G. Polymer 1999, 147, 161.
12. Inoue, T. Prog Polym Sci 1995, 20, 119.
13. Hsieh, Y. N.; Yu, T. L. J Appl Polym Sci 1999, 73, 2413.
14. Schulz, M.; Paul, B. Phys Rev B 1998, 58, 11096.
15. Huang, Y.-J.; Su, C. C. Polymer 1994, 35, 2397.
16. Boyard, N.; Vayer, M.; Sinturel, C.; Erre, R. J Appl Polym Sci 2005, 95, 1459.
17. Suspene, L.; Fourquier, D.; Yang, Y. S. Polym Eng Sci 1991, 30, 1585.
18. Ross, L. R.; Hardebeck, S. P.; Bachmann, M. A. SPI Tech Pap 1988, 17-C.
19. Van Assche, G.; Verdonck, E.; Van Mele, B. Polymer 2001, 42, 2959.
20. Pascault, J. P.; Sautereau, H.; Verdu, J.; Williams, R. J. J. Thermosetting Polymers; Marcel Dekker: New York, 2002.
21. Mortensen, K. J Phys A: Condens Matter 1996, 8, 103.
22. Svensson, M.; Alexandridis, P.; Linse, P. Macromolecules 1999, 32, 637.
23. Mijovic, J.; Shen, M.; Sy, J. W.; Mandragon, I. Macromolecules 2000, 33, 5235.
24. Guo, Q.; Thomann, R.; Gronski, W.; Stavena, R.; Ivanova, R.; Stühn, W. Macromolecules 2003, 36, 3635.
25. Zheng, H.; Zheng, S.; Guo, Q. J Polym Sci Part A: Polym Chem 1997, 35, 3161.
26. Guo, Q.; Harrats, C.; Groeninckx, G.; Koch, M. H. J. Polymer 2001, 42, 4127.
27. Cahn, J. W.; Hilliard, J. E. J Chem Phys 1958, 28, 258.
28. Cook, H. E. Acta Metall 1970, 18, 297.
29. Binder, K. J Chem Phys 1983, 79, 6387.
30. Jinnaï, H.; Hasegawa, H.; Hashimoto, T.; Han, C. C. J Chem Phys 1993, 99, 8154.
31. Li, W.; Lee, L. J. Polymer 2000, 41, 685.
32. Li, W.; Lee, L. J. Polymer 2000, 41, 697.
33. Boyard, N.; Sinturel, C.; Vayer, M.; Erre, R.; Levitz, P. Polymer 2005, 46, 661.
34. Levitz, P. Adv Colloid Interface Sci 1998, 76, 71.
35. Odian, G. Principles of Polymerization, 3rd ed.; Wiley: New York, 1991.
36. Van Assche, G.; Van Hemelrijck, A.; Rahier, H.; Van Mele, B. Thermochim Acta 1996, 286, 209.
37. De la Caba, K.; Guerro, P.; Eceiza, A.; Mondragon, I. Polymer 1996, 37, 275.
38. Boyard, N.; Vayer, M.; Sinturel, C.; Erre, R.; Delaunay, D. J Appl Polym Sci 2004, 92, 2976.
39. Montserrat, S.; Roman, F.; Colomer, P. Polymer 2003, 44, 101.
40. Zetterlund, P. B.; Johnson, A. F. Polymer 2002, 43, 2039.
41. Ramis, X.; Salla, J. M. J Polym Sci Part B: Polym Phys 1999, 37, 751.
42. Kamal, M. R.; Sourour, S. Polym Eng Sci 1973, 13, 59.
43. Schawe, J. E. K. Thermochim Acta 2002, 6950, 1.
44. Francis, B.; Vanden Poel, G.; Posada, F.; Groeninckx, G.; Lakshmana Rao, R.; Ramaswamy, R.; Thomas, S. Polymer 2003, 44, 2687.
45. Barral, L.; Cano, J.; Lopez, J.; Lopez-Bueno, I.; Nogueira, P.; Abad, M. J.; Ramirez, C. J Polym Sci Part B: Polym Phys 2000, 38, 351.
46. Chern, C. S.; Poehlein, G. W. Polym Eng Sci 1987, 27, 788.